DR2012283

SUPPLEMENTARY INFORMATION

A mild Little Ice Age and unprecedented recent warmth in an 1800-year lake sediment record from Svalbard

William J. D'Andrea[1*†], David Vaillencourt[1], Nicholas L. Balascio[1], Al Werner[2], Steven R. Roof[3], Michael Retelle[4], Raymond S. Bradley[1]

[1]*Department of Geosciences, University of Massachusetts Amherst, Amherst, MA, USA*

[2]*Department of Geology and Geography, Mount Holyoke College, South Hadley, MA, USA*

[3]*School of Natural Sciences, Hampshire College, Amherst, MA, USA*

[4]*Department of Geology, Bates College, Lewiston, ME, USA*

[†]*Present address: Lamont-Doherty Earth Observatory of Columbia University, Palisades, NY, USA*

**email: dandrea@ldeo.columbia.edu*

Tephrochronology methods and description

Cryptotephra samples were taken at 2 cm (9–37 cm) and 1 cm (37–47 cm) intervals, treated with HNO_3, heated, washed over a 20 μm sieve, and subjected to liquid density separations (Turney et al., 2006). Sediment 2.3–2.5 g/cm^3 was mounted on microscope slides in epoxy resin, and glass shards were counted using polarizing light microscopy. Select slides were polished to expose grain interiors and analyzed using wavelength dispersive spectrometry on a Cameca SX50 electron microprobe (accelerating voltage 15 keV, beam current 10 nA, beam size of 5–10 μm). Instrument calibration was performed using a series of silicate minerals, synthetic oxides, and glass standards. Results reported are non-normalized major oxide concentrations and only analyses with total weight percent greater than 96% were accepted.

Tephra in core Kong-B consisted of small (20–50 μm), colorless to faint brown, vesicular glass shards (see the Data Repository, Figure DR1) in low concentrations (<98 grains/cm^3). The geochemical data from glass shards within each sample fall into two populations, and the more abundant of each was used to correlate to Icelandic eruptions. Shards of the less abundant, unknown populations are likely reworked tephra grains and are too few in number to serve as confident chronologic markers. The A.D. 1362 eruption of Öræfajökull and A.D. 1104 eruption of Hekla are well constrained by historic documents, and tephra from these eruptions have been identified at a number of sites, providing geochemical reference for tephra in core Kong-B (Wastegård and Davies, 2009) (Table 1). The timing and geochemical composition of the Sn-1 tephra from the Snæfellsjökull volcano in western Iceland, are less well constrained. Sn-1 has been dated to between 1750 ± 150 ^{14}C yr B.P. (ca. 1690 cal yr B.P.) (Steinthorsson, 1967) and 1855 ± 25 ^{14}C yr B.P. (ca. 1780 cal yr B.P.) (Larsen et al., 2002), has a trachydacitic composition, and is characterized by high Al_2O_3 and K_2O values (Larsen et al., 2002). Shards in Kong-B from 39 to 44 cm most strongly resemble this tephra, with minor compositional differences attributable to the compositional variability of tephra produced by this eruption (Larsen et al., 2002; Kristjánsdóttir et al., 2007).

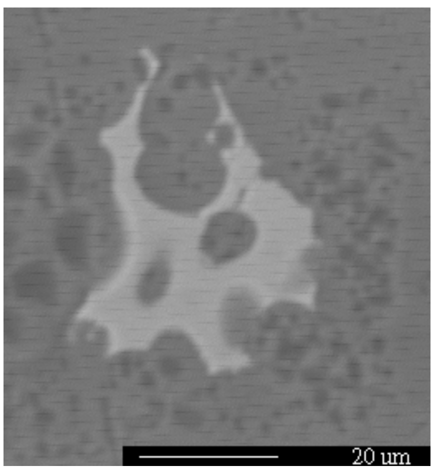

Figure DR1. Cryptotephra. Image of a tephra shard recovered from sediment core Kong-B and used for geochemical measurements and tephrochronology.

Alkenone methods and U_{37}^{K} calibration development

Alkenone samples were taken at 0.25 cm intervals from the sediment surface to a depth of 19 cm and at 0.5 cm intervals for the remainder of the core resulting in temporal resolution ranging 5-40 years due to changes in sampling resolution and sedimentation rate (Fig. 2). Samples were freeze-dried, homogenized, and extracted with 9:1 dichloromethane:methanol by ASE200 (Dionex). Extracts were dried, saponified at 75 °C for 12 h with 0.5M KOH in 95% methanol/H_2O, and lipids extracted with toluene. Alkenones were quantified by gas chromatography-flame ionization detection (HP6890

Series). U_{37}^{K} was measured with precision of ± 0.007 (±1σ), determined with an alkenone standard analyzed every 10 sample injections.

Samples for the U_{37}^{K} calibration were obtained by extruding and collecting (0.25 cm intervals) the upper sediments of core Kong-B in the field immediately following core recovery. The core was maintained in an upright position after recovery to prevent any turbulent mixing of the sediments. Samples representing the calibration period (A.D. 1921-2009; n=15) ranged from having 3 to 11 years of sediment accumulation due to the constant sampling interval (0.25 cm) and changing sedimentation rate. We determined the years of sedimentation represented by each of our samples according to the ^{210}Pb and $^{239+240}Pu$ age model and resampled the air temperature record from Longyearbyen Airport (Nordli, 2010) by calculating average June/July/August air temperatures for each time interval (Fig. 2C,D). Linear regression was used to compare the resampled air temperature data with the U_{37}^{K} values measured from the sediment samples and to determine the calibration (U_{37}^{K} = 0.0255 (T) – 0.804; r^2 = 0.59; n = 15; $p < 0.001$).

Table DR1. Calibration data

UK37	Period of sedimentation (yrs A.D.)	JJA Temp (°C)*
-0.654	2006-2009	5.8
-0.674	2003-2005	5.7
-0.649	1998-2002	5.3
-0.668	1992-1997	4.5
-0.693	1989-1991	4.6
-0.680	1985-1988	4.7
-0.706	1980-1984	3.9
-0.682	1972-1979	4.4
-0.695	1963-1971	3.9
-0.700	1956-1962	4.3
-0.691	1949-1955	4.3
-0.699	1944-1948	3.9
-0.721	1936-1943	4.2
-0.709	1927-1935	4.5
-0.687	1915-1926	4.4

*June/July/Air temperatures from Nordli, 2010

Table DR2. Major oxide concentration of individual tephra shards from core Kong-B.

No.	SiO_2	TiO_2	Al_2O_3	FeO	MnO	MgO	CaO	Na_2O	K_2O	Cl	Total
19-21 cm, Group 1 - Unknown											
1	70.69	0.24	13.81	3.21	0.09	0.15	1.93	3.52	2.52	0.11	96.29
2	68.30	0.25	15.26	3.17	0.16	0.10	1.12	4.68	4.37	0.28	97.74
3	68.22	0.25	14.84	3.12	0.12	0.10	1.06	4.72	4.57	0.27	97.24
4	68.46	0.26	14.43	3.00	0.15	0.08	1.09	4.65	4.25	0.28	96.64
19-21 cm, Group 2 - Öræfajökull AD 1362											
1	70.69	0.25	13.53	3.40	0.06	0.01	0.94	5.00	3.29	0.19	97.36
2	73.64	0.25	13.43	3.25	0.10	0.00	0.93	4.50	3.53	0.21	99.86
3	72.33	0.23	13.09	3.23	0.11	0.02	0.97	4.68	3.51	0.21	98.39
4	71.48	0.20	13.07	3.26	0.07	0.00	0.95	4.77	3.31	0.22	97.33
5	70.17	0.22	13.11	3.05	0.08	0.00	0.91	4.93	3.43	0.22	96.16
6	70.80	0.24	13.41	3.17	0.08	0.00	0.93	4.70	3.31	0.21	96.89
7	71.79	0.22	13.26	3.15	0.09	0.00	0.93	4.75	3.19	0.23	97.63
8	72.98	0.24	13.39	3.32	0.10	0.00	0.93	4.63	3.40	0.20	99.19
9	72.13	0.23	13.19	3.28	0.07	0.00	0.93	4.68	3.30	0.23	98.05
10	71.36	0.18	13.05	3.27	0.07	0.00	0.89	4.95	3.25	0.22	97.23
11	72.32	0.22	13.36	3.21	0.09	0.00	0.93	4.82	3.33	0.21	98.49
12	72.96	0.22	13.24	3.24	0.10	0.00	0.91	4.81	3.42	0.28	99.19
13	72.13	0.22	13.22	3.34	0.06	0.00	0.94	4.48	3.30	0.25	97.95
14	71.74	0.20	13.14	3.19	0.04	0.00	0.89	4.54	3.28	0.22	97.24
15	72.24	0.22	13.40	3.21	0.08	0.00	0.93	3.72	3.28	0.18	97.26
Avg	71.92	0.22	13.26	3.24	0.08	0.00	0.93	4.66	3.34	0.22	97.88
1 σ	0.93	0.02	0.15	0.08	0.02	0.01	0.02	0.30	0.10	0.02	0.99
27-29 cm, Group 1 - Unknown											
1	70.89	0.22	15.17	3.08	0.17	0.09	1.00	4.41	4.50	0.27	99.78
2	68.84	0.28	15.32	3.11	0.14	0.08	1.06	4.34	4.46	0.27	97.94
3	69.83	0.20	14.82	2.98	0.14	0.00	0.89	5.19	4.42	0.23	98.69
27-29 cm, Group 2 - Hekla AD 1104											
1	71.40	0.18	14.05	3.34	0.08	0.11	2.05	3.95	2.63	0.08	97.89
2	70.41	0.20	13.72	3.37	0.08	0.10	1.85	4.45	2.55	0.09	96.83
3	73.39	0.21	14.30	3.37	0.09	0.10	1.93	3.87	2.56	0.04	99.90
4	70.69	0.20	13.99	3.22	0.09	0.06	1.91	4.61	2.54	0.05	97.33
5	70.76	0.22	13.96	3.44	0.18	0.12	1.93	4.53	2.60	0.07	97.82
6	69.98	0.24	14.05	3.49	0.12	0.11	1.97	4.46	2.52	0.05	97.00
7	72.71	0.19	14.27	3.21	0.12	0.13	2.05	3.80	2.57	0.07	99.11
8	71.96	0.19	14.11	3.11	0.09	0.08	1.93	3.82	2.61	0.06	98.02
9	70.43	0.14	14.01	3.34	0.15	0.13	2.01	4.50	2.65	0.08	97.44
10	71.40	0.14	14.13	3.27	0.12	0.12	1.90	4.77	2.66	0.06	98.64
11	72.41	0.22	14.08	3.06	0.13	0.07	1.98	4.12	2.50	0.07	98.70
12	69.59	0.19	14.14	3.32	0.11	0.09	1.90	4.67	2.55	0.06	96.68
13	70.98	0.20	14.35	2.89	0.11	0.07	2.06	3.57	2.43	0.06	96.75
14	71.84	0.20	14.26	3.17	0.08	0.12	1.88	4.52	2.57	0.04	98.67
15	71.69	0.27	13.83	3.30	0.09	0.10	1.96	4.72	2.61	0.05	98.63
16	71.67	0.23	14.47	3.30	0.09	0.11	1.92	3.87	2.66	0.06	98.38
17	70.86	0.23	13.94	3.35	0.12	0.06	1.91	4.80	2.66	0.06	98.03
18	70.27	0.18	13.79	3.25	0.13	0.08	1.97	4.57	2.54	0.07	96.86
19	71.63	0.20	14.16	3.26	0.09	0.14	1.87	4.60	2.71	0.05	98.70
20	70.33	0.16	13.72	3.42	0.10	0.14	1.87	4.63	2.58	0.05	96.98
21	71.59	0.22	13.29	3.21	0.08	0.01	1.52	4.42	2.64	0.06	97.03
Avg	71.24	0.20	14.03	3.27	0.11	0.10	1.92	4.35	2.59	0.06	97.87
1 σ	0.95	0.03	0.26	0.14	0.03	0.03	0.11	0.38	0.07	0.01	0.91

					39-44 cm, Group 1 - Unknown						
1	72.81	0.32	13.24	1.17	0.00	0.29	1.05	3.54	2.86	0.16	95.44
2	69.42	0.37	13.40	1.48	0.04	0.45	1.65	3.38	2.80	0.19	93.18
3	71.70	0.27	12.96	1.17	0.00	0.26	1.08	3.32	2.90	0.16	93.81
4	70.08	0.46	15.07	1.99	0.03	0.53	1.83	4.28	2.58	0.17	97.01
5	73.83	0.28	13.34	1.20	0.04	0.27	1.10	3.59	2.81	0.17	96.63
6	73.63	0.29	13.58	1.40	0.00	0.31	1.11	3.40	2.80	0.14	96.65
7	72.83	0.38	14.36	1.66	0.03	0.47	1.61	2.99	2.69	0.17	97.18
Avg	72.04	0.34	13.71	1.44	0.02	0.37	1.35	3.50	2.77	0.17	95.70
1 σ	1.72	0.07	0.74	0.31	0.02	0.11	0.33	0.40	0.11	0.02	1.62
					39-44 cm, Group 2 - Sn-1 c. AD 170						
1	68.75	0.21	15.49	3.25	0.11	0.12	0.94	3.76	4.45	0.23	97.30
2	68.45	0.21	15.32	3.22	0.09	0.13	1.04	4.22	4.46	0.29	97.41
3	68.97	0.22	15.54	3.15	0.14	0.07	1.03	3.62	4.38	0.25	97.37
4	68.76	0.22	15.51	3.14	0.08	0.10	0.98	3.17	4.48	0.24	96.68
5	69.01	0.26	15.35	3.45	0.04	0.12	1.10	3.33	4.38	0.26	97.30
6	68.69	0.26	15.44	3.15	0.12	0.09	0.93	3.15	4.46	0.28	96.56
7	68.57	0.25	15.57	3.15	0.03	0.11	0.99	3.55	4.49	0.25	96.95
8	68.19	0.29	15.44	3.34	0.12	0.12	1.13	4.83	4.39	0.26	98.11
9	68.19	0.29	15.12	3.00	0.14	0.08	1.05	4.31	4.59	0.25	97.02
10	70.17	0.23	15.39	3.04	0.11	0.09	1.02	4.30	4.54	0.25	99.13
11	68.08	0.31	15.51	3.33	0.15	0.09	1.19	4.61	4.40	0.25	97.91
12	68.18	0.23	15.34	3.15	0.11	0.07	1.07	4.61	4.48	0.23	97.47
13	69.69	0.26	15.38	3.31	0.12	0.09	1.02	3.67	4.37	0.29	98.19
14	66.69	0.29	15.71	3.35	0.11	0.14	1.10	4.63	4.22	0.26	96.49
15	68.18	0.30	15.77	3.58	0.13	0.21	1.20	3.18	4.30	0.25	97.10
16	67.74	0.19	15.40	3.14	0.13	0.10	0.98	4.43	4.47	0.25	96.82
17	68.44	0.27	15.42	3.11	0.11	0.13	0.95	4.42	4.52	0.26	97.61
18	68.60	0.23	15.57	3.23	0.12	0.11	1.02	3.77	4.59	0.23	97.46
19	67.91	0.24	15.33	3.08	0.10	0.12	1.04	4.57	4.34	0.24	96.97
20	67.73	0.23	15.37	3.21	0.14	0.06	1.01	4.45	4.50	0.26	96.96
21	66.85	0.26	15.43	3.36	0.13	0.12	1.16	4.22	4.41	0.28	96.21
22	67.10	0.40	16.10	4.11	0.17	0.31	1.60	3.66	4.15	0.24	97.83
23	67.76	0.25	15.26	3.20	0.13	0.13	1.08	4.42	4.42	0.25	96.89
24	67.70	0.21	15.65	3.09	0.13	0.07	0.95	4.32	4.37	0.26	96.75
25	67.71	0.22	15.62	3.12	0.15	0.11	1.04	3.44	4.49	0.26	96.16
26	67.18	0.22	15.47	3.25	0.11	0.11	0.99	4.40	4.45	0.24	96.42
27	67.69	0.24	15.27	3.29	0.10	0.10	1.03	4.00	4.43	0.27	96.43
28	68.89	0.27	15.10	2.96	0.09	0.10	0.95	3.84	4.65	0.25	97.09
Avg	68.21	0.25	15.46	3.24	0.11	0.11	1.06	4.03	4.43	0.25	97.16
1 σ	0.79	0.04	0.20	0.22	0.03	0.05	0.13	0.51	0.11	0.02	0.66

Table DR3. Age markers used as input to Clam-based age model (Blaauw, 2010) and Clam-based error estimates. The age model for core Kong-B was developed using Clam v. 1.0.2 (Blaauw, 2010). It utilizes 14 age markers, including the core top, nine ^{210}Pb dates (Appleby and Oldfield, 1978), the AD 1963 $^{239+240}$Pu spike resulting from the 1963/1964 fallout from nuclear weapons testing (Ketterer et al., 2004) and tephra from three volcanic eruptions detailed above. The Clam model was run as a smooth spline (type 4) with a smoothing value of 0.3 and 10,000 iterations, allowing for the greatest amount of flexibility without producing age reversals. The 95% confidence intervals around individual age markers range from 1 to 210 years (average of 67 years) evaluated every 0.25 cm.

Chronological marker	Sample depth (cm)	Sample thickness (cm)	Age (years before 1950)	^{14}C Age	Clam error estimate (yrs)
Core top	0	0.1	-59	-	1
^{210}Pb	0.5	0.5	-53.5	-	0.7
^{210}Pb	1	0.5	-44.3	-	0.9
^{210}Pb	1.5	0.5	-39.4	-	1.0
^{210}Pb	2	0.5	-30.4	-	1.2
^{210}Pb	2.5	0.5	-13.0	-	1.9
^{210}Pb	3	0.5	1.5	-	2.7
^{210}Pb	3.5	0.5	8.5	-	3.2
^{210}Pb	4	0.5	22.7	-	4.5
^{210}Pb	4.5	0.5	46.6	-	8.2
$^{239+240}$Pu	2.5	0.25	-13	-	3
Öræfajökull eruption	20	2	588	-	10
Hekla eruption	28	2	846	-	10
Snæfellsjökull eruption	43.5	1	-	1855	25

Equation DR1. The standard error of estimation for the U^{K}_{37} -temperature calibration was calculated with the following formula:

$$SE = \sqrt{\frac{1}{(n-2)}[\sum(y-\bar{y})^2 - \frac{[\sum(x-\bar{x})(y-\bar{y})]^2}{\sum(x-\bar{x})^2}]}$$

where, n = sample size; $\bar{x}$ and $\bar{y}$ are sample means.

REFERENCES CITED

Appleby, P.G., and Oldfield, F., 1978, The calculation of lead-210 dates assuming a constant rate of supply of unsupported 210Pb to the sediment: Catena, v. 5, p. 1-8.

Blaauw, M., 2010, Methods and code for 'classical' age-modelling of radiocarbon sequences: Quaternary Geochronology, v. 5, p. 512-518.

Ketterer, M.E., Hafera, K.M., Jones, V.J., and Appleby, P.G., 2004, Rapid dating of recent sediments in Loch Ness: inductively coupled plasma mass spectrometric measurements of global fallout plutonium: Science of the Total Environment, v. 322, p. 221-229.

Kristjánsdóttir, G.B., Stoner, J.S., Jennings, A.E., Andrews, J.T., and Grönvold, K., 2007, Geochemistry of Holocene cryptotephras from the North Iceland Shelf (MD99–2269): Intercalibration with radiocarbon and paleomagnetic chronostratigraphies: The Holocene, v. 17, p. 155–176, doi:10.1177/0959683607075829.

Larsen, G., Eiríksson, J., Knudsen, K.L., and Heinemeier, J., 2002, Correlation of late Holocene terrestrial and marine tephra markers, north Iceland: implications for reservoir age changes: Polar Research, v. 21, p. 283–290, doi:10.1111/j.1751-8369.2002.tb00082.x.

Nordli, Ø., 2010, The Svalbard Airport Temperature Series: Bulletin of Geography: Physical Geography Series, v. 3, p. 5–25.

Steinthorsson, S., 1967, Tvær nýjar 14C-aldursákvardanir á öskulögum úr Snæfellsjökli: Náttúrufrœdingurinn, v. 37, p. 236–238.

Turney, C.S.M., van den Burg, K., Wastegård, S., Davies, S.M., Whitehouse, N.J., Pilcher, J.R., and Callaghan, C., 2006, North European last glacial-interglacial transition (LGIT; 15–9 ka) tephrochronology: Extended limits and new events: Journal of Quaternary Science, v. 21, p. 335–345, doi:10.1002/jqs.990.

Wastegård, S., and Davies, S.M., 2009, An overview of distal tephrochronology in northern Europe during the last 1000 years: Journal of Quaternary Science, v. 24, p. 500–512, doi:10.1002/jqs.1269.